Combining spring wheat genotypes with contrasting root architectures for a better use of water resources in soil? Evidence from column-scale water stable isotopic experiments

Samuel LE GALL

s.le.gall@fz-juelich.de

Forschungszentrum Julich ICG: Forschungszentrum Julich GmbH https://orcid.org/0000-0001-6280-5048

Dagmar van Dusschoten
Adrian Lattacher
Mona Giraud
Moritz Harings
Paulina Deseano Diaz
Daniel Pflugfelder
Samir Alahmad
Lee Hickey
Ahmet Sircan
Ellen Kandeler
Guillaume Lobet
Andrea Schnepf
Holger Pagel
Christian Poll
Harry Vereecken
Mathieu Javaux
Youri Rothfuss

Research Article

Keywords: Wheat mixture, water stable isotopes, water deficit, root architecture, root water uptake plasticity.

Posted Date: September 4th, 2025

DOI: https://doi.org/10.21203/rs.3.rs-7411150/v1

Abstract

Background and Aims

The advantages of genotype mixtures on soil water balance are still poorly understood. We aim to determine the impact of soil water conditions (well-watered or chronic water deficit) on the root water uptake (RWU) of two contrasting root genotypes and their mixture at the booting stage.

Methods

We conducted a controlled plant-soil column experiment and quantified daily vertical profiles of the fraction of RWU (fRWU, % cm^{-1}), i.e. the relative contribution of RWU normalized by the thickness of each layer. This calculation was achieved by applying Bayesian modelling on non-destructive soil and transpiration water stable isotopic measurements after pulse labelling. We compared these results to the monitored plant soil water status, plant physiology and root architectures.

Results

The "shallow-rooted" genotype exhibited a greater fRWU compared to the "deep-rooted" genotype in the topsoil (3.87 ± 1.05 and 3.49 ± 1.05% cm^{-1}, respectively) and vice-versa for the subsoil (resp. 1.16 ± 0.17 and 1.53 ± 0.41% cm^{-1}). The relative water uptake of all plant modalities from subsoil (+ 0.5% cm^{-1}) and topsoil (+ 0.29% cm^{-1}) increased under water deficit conditions. The genotype mixture maintained individual complementary fRWU distribution but shifted their contributions toward the subsoil (+ 0.5% cm^{-1}) and decreased those from the topsoil (-1.2% cm^{-1}) under water deficit.

Conclusion

This study introduces novel observations of root water uptake plasticity, which is determined by genotype root architectures, soil water availability, and interactions with neighboring plant root architectures. This study highlights the potential of contrasting root architectures mixtures to improve their water - and nutrient – access facing water deficit.

1 Introduction

One potential strategy for agriculture to maintain high yields and ensure the soil health in the context of climate change involves the (re)introduction of greater biodiversity to agroecosystems (Altieri et al. 2017; Messéan et al. 2021). At the landscape scale, this can be achieved through the implementation of hedges, patchwork cultivation, or grass strips (Vanneste et al. 2020). At the field scale, biodiversity enhancement can be achieved through the implementation of diverse crop rotations, which may

encompass various cultivation cycles of different duration, such as perennial grain (Duchene et al. 2020). Between cycles of the crop of interest, the introduction of catch crop or cover crop can be a complementary practice (Moreau et al. 2012; Vincent-Caboud et al. 2019). Biodiversity can also be cultivated within the same time and space, for example through the implementation of agroforestry systems, which combine large perennial and small annual plants (Mettauer et al. 2023; Nerlich et al. 2013). Alternatively, different annual crops can be grown in the same field, a practice known as intercropping, blending or maslins (Blanc et al. 2024; Brooker et al. 2015; Duchene et al. 2017; Hawes et al. 2021). These practices have been evidenced to engender beneficial effects in terms of crop pollination, to diminish pest pressure and to enhance crop yield stability and quality, especially under non-optimum water and nutrient conditions (Chabert et al. 2024; Francesco Giovanni Salvo et al. 2022; Gaba et al. 2015; McAlvay et al. 2022; Schöb et al. 2023). However, the necessity for specific technical itineraries, inputs (fertilizer, phytosanitary, etc.) and adapted machinery to account for differences in physiological development of the associated species are significant obstacles to the implementation of co-cropping, especially in Europe (Brannan et al. 2023; Bybee-Finley and Ryan 2018; Wezel et al. 2014). A promising yet less well-studied alternative to adding more inter-specific plant diversity to agroecosystems is to take advantage of the existing intra-specific crop biodiversity (Albert et al. 2011; Bruelheide et al. 2018; Jung et al. 2010; Litrico and Violle 2015).

Wheat occupies a central place in global food production and its yield is sensitive to climate change (Ortiz et al. 2008; Wilcox and Makowski 2014). Consequently, wheat genotype mixtures have gained interest over the last decades due to higher epidemiologic resistance, leading to more stable yields or even higher production. The combination of these advantages, along with the relative ease with which they can be adapted to different farming techniques, compared to inter-specific mixtures (also named co-cropping), has led to an increased interest to farmers (Perrone et al. 2017). However, the mixing of random genotype diversity alone is not a sufficient criterion for the design of efficient mixtures (Lamichhane et al. 2018). In order to propose a clear overview of the possibilities and outcomes for farmers, the principles to design mixtures, trait-based or trait-blind, need to be studied (Barot et al. 2017). While a significant proportion of plant-plant interactions occurs beneath the soil, these interactions have often been overlooked in research (Homulle et al. 2022). The extant literature highlights the necessity of (i) a comprehensive understanding of the underlying mechanisms of the ecosystem services observed and (ii) the identification of the trait configurations that lead to both high performance and stability of the mixture over time (Demie et al. 2022; Hughes et al. 2008; Lecarpentier et al. 2019).

Within these mechanisms, the strategies and patterns of root water uptake, in addition to the nutrients contained therein, are of critical importance to the plant's adaptation to water deficit. Water uptake is determined by the hydraulic soil-plant-atmosphere gradient and is further regulated by the root architectures, such as architecture, rooting depth and density distribution, as well as root and microbial exudation (Doussan et al. 2024; Freschet et al. 2021; Giraud et al. 2023). Research has demonstrated that deep-rooting wheat genotypes enhance grain yield under water deficit conditions (El Hassouni et al. 2018; Nakhforoosh et al. 2014; Wasson et al. 2012) and have associated these outcomes with enhanced water use efficiency (Feng et al. 2017; Hafeez et al. 2024). Root plasticity also enables plants to adapt

their root architectures and their water uptake to optimize water uptake under water-deficit conditions, shifting it either more toward the subsoil (Wang et al. 2024; Xu et al. 2016) or the topsoil (Shazadi et al. 2024). However, the interaction between contrasting wheat root architectures genotypes in a cropped mixture and their divergent root water uptake strategies remains to be fully understood.

The objective of this study was to assess whether the combination of wheat genotypes with contrasting root architectures can improve water supply to the plant population. We focused on the booting stage because it is crucial for yield determination, involving the stabilization of the number of fertile spikes and flower formation, as well as the development of grain filling potential (Fischer 1985; Wu et al. 2022; Xu et al. 2022). We hypothesize that two selected genotypes exhibit significantly different root water uptake (RWU) patterns at this key development stage. Particularly under water deficit conditions, we expect a relatively higher RWU of a shallow-rooted genotype from topsoil in comparison to a deep-rooted genotype, which shows relatively higher root water uptake from subsoil. Water deficit conditions are expected to shift the primary RWU to subsoil and wetter layers. When the two genotypes are grown as a mixture, we assume that their complementary water absorption profiles will enable both plants to cope better with water-deficit conditions.

Our study uses a controlled plant-soil column experiment to analyze the water use of two wheat genotypes with similar root biomass and contrasting root angle of insertion in the early stages of development (Rambla et al. 2022). Root architectures of these genotypes also exhibit contrasting traits in later stages of development (Lattacher et al. 2025a). We estimated the root water uptake patterns of the wheat genotypes grown in monocultures and mixtures under well-watered (WW) and water deficit (WD) conditions using stable water isotope labeling and tracing. Based on this experimental evidence, we then discuss the inter-genotype plasticity of root water uptake patterns and potential benefits of cropping wheat genotype mixtures to cope with water deficit.

2 Materials and methods

2.1 Experimental setup

For the study, soil columns with an internal diameter of 11 centimeters and a height of 80 centimeters were used. These columns contained air-dried soil with a silt loam texture containing 22% clay, 66% silt, and 12% sand (Weihermüller et al. 2007) that had been sieved to a mesh size of 2 millimeters, collected from the upper 30cm an agricultural field (Haplic luvisol) in Selhausen, Germany (50°52'07.8" N, 6°26'59.7" E). The soil within the columns was compacted using a vibrating plate (Haver EML 450 Digital Plus N, Haver & Boecker, Oelde, Germany) to attain a homogeneous dry bulk density of 1.4 g cm^{-3} across the entire soil column. This density is representative of field conditions measured on average in the origin agricultural field. Subsequently, the soil of all columns was saturated with water from below via a porous plate. Then the soil columns were covered for a period of two weeks to prevent evaporation and to establish a stable level of homogeneous hydraulic status and microbial activity within the entire

column. Thereafter, four pre-germinated sprouts were placed within each column and some days later, the two less vigorous were removed.

Two experimental spring wheat (*Triticum aestivum L.*) lines, UQR012 (shallow-rooted architecture : SRS) and UQR015 (deep-rooted architecture : DRS), with strongly contrasting seminal root angles, determined at early growing stage, were used (Rambla et al. 2022). The genotypes were developed by backcrossing a donor source for narrow root angle to the high-yielding spring wheat genotype Borlaug100 (Rambla et al. 2022). The plants were grown in monoculture (SRS or DRS) and mixture (MIX) in a climate chamber under controlled conditions.

From the sowing time on, water was applied to the topsoil using two different watering treatments. Watering regimes were adjusted to varying intensities, targeting for the 6th week of growth a matric potential corresponding to a pF value of 2.0–3.0 for the "well-watered" (WW) treatment and a pF value of 3.5–4.5 for the "water deficit" (WD) treatment. The watering for the WW treatment represented a total quantity of about 1300 mL of water over 6 weeks of growth, equivalent to 137 mm of rainfall, approaching the 10-year average of rainfall accumulated over 6 weeks between March and May in Selhausen (Zoomash). For the WD treatment, only 200 ml of water was applied over the same growth period, equivalent to 21 mm of rainfall, similar to two of the dry spring months in 2021 or 2022, to achieve chronic and progressive water deficit (Lynch, 2018). Evaporation from the topsoil was minimized by covering it with a plastic film during the experiment. This resulted in the following plant modalities and water treatments combinations: WW-SRS, WW-DRS, WW-MIX, WD-SRS, WD-DRS and WD-MIX. Each combination was replicated over nine soil columns replicates, which were generated in six separate runs due to the spatial limitation of the climate chamber. Each of the nine replicates include three soil columns for the water stable isotopic measurements (Acrylic columns) and six soil columns for NMR measurements (PVC columns) (Fig. 1).

The Acrylic columns were specifically designed to include gas probes (KM-PPMF-055-00-000-0000-0, 0.155 cm wall thickness, 0.55 cm i.d., 0.86 cm o.d., 0.2 µm pore size; Katmaj Filtration®, Poland) for the online and non-destructive determination of the soil water vapor δ^2H and $\delta^{18}O$ (Rothfuss et al. 2013). We also installed soil matric potential (SMP, MPa) and temperature (T, °C) sensors (Teros 21, Meter, München, Germany) (Fig. S1). The acrylic columns were complemented by six polyvinyl chloride (PVC)-made columns of the exact same dimensions. These columns did not include any metal parts or metal-built sensors, which allowed for the visualization of the root architecture with magnetic resonance imaging (MRI) at the 6th week of plant growth. The PVC column plants (MRI measurements) were grouped into sets of three columns in a single gas exchange chamber three times larger than an individual chamber (79 L in volume, 33 cm in width, 40 cm in height and 60 cm in length).

In the climate chamber, air temperature was set to 20 ± 0.22°C, relative humidity was set to 50.0 ± 2%. Light was provided with homemade LED panels (LEDs:CXA2520-0000-000N0YN430H, Lighting Solutions, Ludenscheid, Germany) cooled with a water bath (RP1845, LAUDA, Germany). The light

intensity followed a sinusoidal-like 24-hour cycle from 0 µmol m-2 s-1 at "night" (from 8 pm to 6 am) to 1200 µmol m-2 s-1 at "midday" (1 pm).

The thermal insulation of the soil column sides allowed the establishment of a soil temperature gradient as would be observed in field conditions, with 2°C higher values in the topsoil layers than lower values in the subsoil layers. In the transpiration chambers, no significant differences were observed between the cultivation modalities and the water treatment in terms of air humidity (74 ± 9%), air temperature (24.0 ± 0.8°C) and vapor pressure deficit (VPD) (0.78 ± 0.27) (Table 1).

A mineral fertilization, equivalent to 60 kg N ha-1, was applied in each soil column at the three leaves-stage. The growth period was restricted to 6 weeks (until 43 days after seeding – DaS) when the plants reached ear emergence from boot, equivalent to Z51-59 on the Zadoks scale (Zadoks et al. 1974).

Table 1 *Mean and standard deviation (sd) resulting of environmental parameters of the experiment in the afternoon between 1 and 3pm at the booting stage (between 39 and 43 DaS) (air temperature in °C; air humidity in %, vapor pressure deficit (VPD) in kPa, pF matric potential and soil temperature in °C) for each culture type, genotype and water treatment (n = 3).*

			Air temperature (°C)		Air humidity (%)		VPD (kPa)		pF		Soil temperature (°C)	
Culture type	Genotype	Water treatment	mean	sd	mean	sd	mean	sd	mean	sd	mean	sd
Monoculture	DRS	WD	24.3	0.9	68%	10%	0.92	0.31	3.6	0.3	20.9	0.7
Mixture	DRS	WD	24.2	0.4	71%	12%	0.88	0.33	3.7	0.3	21.1	0.6
	SRS	WD	24.4	0.2	76%	11%	0.72	0.32				
Monoculture	SRS	WD	24.3	0.7	69%	8%	0.91	0.27	3.6	0.5	21.1	0.7
Monoculture	DRS	WW	23.4	0.6	79%	4%	0.65	0.13	2.8	0.4	21.1	0.9
Mixture	DRS	WW	24.4	0.8	73%	7%	0.82	0.23	2.9	0.8	21.4	0.5
	SRS	WW	24.5	0.7	76%	5%	0.73	0.15				
Monoculture	SRS	WW	23.8	0.6	78%	5%	0.68	0.14	2.6	0.6	21.0	0.7

2.2 Labeling strategy, water stable isotopic monitoring, and RWU determination

Labeling was conducted to increase the precision of the RWU estimates. The labeling approach was designed to lead to 1) diverging vertical profiles in soil water δ^2H and $\delta^{18}O$; 2) to the increase in soil water δ^2H and $\delta^{18}O$ gradients across depth and 3) to a non-significant rise in soil water content value. This was done by adding small amounts (10 ml) of isotopically labeled water ($-149.0‰ < \delta^2H < 1026.0‰$, $-302.0‰ < \delta^{18}O < 96.0‰$) at 0, 20, 40, 60, and 80cm depth via perforated tubing (Synflex "1300" 1/4", Eaton, Dublin, Ireland) at 28 and 34 DaS, in order to achieve contrasting isotopic composition profiles later between 39 and 42 DaS for estimating the fRWU. The targeted $\delta^{18}O$ profile was monotonic and ranged from − 20‰ (80 cm) to + 70‰ (0 cm). Contrarily for δ^2H, we targeted a non-monotonic, V-shaped profile increasing from − 70‰ at 80 cm to + 170‰ at 40 cm and decreasing again towards the topsoil to − 70‰.

The weight loss in the acrylic columns was recorded (IFS60K0.5D, Kern, Balingen, Germany) throughout the experiment to calculate the transpiration rate gravimetrically. In the sixth and final week of each experimental series, plant transpiration rate (Tr, mL/min) and transpiration isotopic composition values δ^2H_{Tr} and $\delta^{18}O_{Tr}$ (δ_{Tr}) were measured on the acrylic column plants, following the method described in Deseano Diaz et al. (2023). For this we used a gas exchange chamber (29 cm diameter, 40 cm length, 27 L volume) that was connected to a laser spectrometer (L2130-i, Picarro Inc. Santa Clara, USA) (Fig. S2) for 20 minutes per plant during the afternoon between 12 and 3 pm to measure maximum water flux (due to maximum light radiation at 1 pm).

We sampled soil water vapor (swv) for 13 minutes at 13 depths (1, 3, 5, 8, 18, 20, 40, 42, 62, 64, 74, 77 and 79cm depth) in the acrylic columns with gas-permeable probes (Fig. 1). The probes were flushed, further diluted with dry synthetic air (at 70 and 30 ml min^{-1}, respectively; GF40 mass flow controller, Brooks Instruments, Hatfield, USA), and analyzed online with a laser spectrometer (L2130-i, Picarro Inc., Santa Clara, USA) for isotopic analysis (δ^2H_{swv} and $\delta^{18}O_{swv}$). δ^2H_{soil} and $\delta^{18}O_{soil}$ (δ_{soil}) were assessed from δ^2H_{swv} and $\delta^{18}O_{swv}$ readings considering thermodynamic equilibrium between soil water vapor and liquid phases according to Rothfuss et al. (2013) (Fig. S2). Data acquisition at a 30-s time resolution as well as the flushing and dilution of the soil gas probes and gas-exchange chambers were automatized in LabView® (NI™, Austin, USA). The raw isotopic data was calibrated following Deseano Diaz et al. (2023)d hnhammer et al. (2020) against two soil water vapor standards (δ^2H_{st1} = 102.4 ± 1.4‰ and $\delta^{18}O_{st1}$ = 30 ± 0.3‰, δ^2H_{st2} = − 78.4 ± 0.6‰ and $\delta^{18}O_{st2}$ = − 18.8 ± 0.1‰).

The gas exchange chambers were fitted with the same relative humidity and air temperature sensors (RFT-2, precision for $RH_{chamber}$ and $T_{chamber}$ = 2% and 0.1°C, respectively; METER Group, Munich, Germany) and fans (500F, DC-Axiallüfter, ebm-papst, Mulfingen, Germany). The acrylic column plant chambers were constantly supplied with 6 to 12 l min^{-1} of air taken from the climatic chamber (T_{cc} = 20 ± 0.22°C, RH_{cc} = 50.0 ± 2%) (Fig. 1). Measurements of relative air humidity ($RH_{chamber}$, %) and air temperature ($T_{chamber}$, °C) in the gas exchange chambers were used to calculate the vapor pressure deficit (VPD, kPa).

Daily-resolved depth profiles of the relative contribution of RWU to plant transpiration, normalized by the thickness of each layer (fraction of Root Water Uptake; fRWU), were computed from 39 to 42 DaS using the multi-source mixing model Stable Isotope Analysis in R (SIAR) (Parnell et al. 2010) following the method of Couvreur et al. (2020) and Deseano Diaz et al. (2023). These estimates on soil liquid water (δ_{soil}) and transpired water vapor (δ_{Tr}) isotopic compositions, assumed steady state transpiration yielding to $\delta_{Tr} = \delta_{RWU}$. For each ‘plant modality x water treatment’ combination, we had three repetitions of columns measured over four successive days, giving a maximum of twelve fRWU profiles per combination, except when a technical problem during the measurement hindered us from obtaining either the soil profile or the plant transpiration data. The fRWU contribution from 18 and 20; 40 and 42,

62 and 64 cm depth were grouped together to better represent respectively the soil layers 14–30, 30–52, 52–69 cm.

The Sink Term (mL min^{-1} cm^{-1}) was calculated as the product of the fRWU (cm^{-1}) and the transpiration rate (mL min^{-1}) calculated from the water vapor mixing ratio measured with the Picarro laser spectrometer, according to the plant transpiration rate formula in Deseano Diaz et al. (2023).

2.3 Aboveground physiological measurement and root architecture

The number of leaves and tillers, the dimensions of the blades (length and width) and sheaths (diameter and length) as well as leaf blade chlorophyll content (SPAD 502Plus, Konica Minolta, Munich, Germany) were manually and non-destructively measured twice a week during growth. We related the transpiration to the total leaf area by adding the area of both sides of the leaves' blades and sheaths, although the latter is close to negligible compared to the former. The leaf blade surface area was calculated considering the measured length of each leaf blade, a constant increasing leaf width over times inferred from regular measurements points, and a coefficient of 0.75 to take into account the oblong wheat leaf shape (Chanda and Singh 2002). The leaf sheath surface was calculated considering it as a cylinder with an average diameter of 5mm and a length equal to the maximum leaf sheath-distance of each tiller. The stomata density was obtained by destructively sampling the flag leaf, applying a nail polish to the bottom part and counting the number of stomata on the nail polish impression with a stereo microscope (Axiophot 2, Zeiss, Germany) (Pathoumthong et al. 2023).

During the 4th and 6th week of plant growth, the root architectures of the plants in the six PVC columns were monitored non-destructively using a 4.7 T MRI magnet (Magnex, Oxford, UK) and a MR Solutions console (Guildford, UK). We constructed a linear axis on top of the magnet to handle these long and heavy soil columns (16 kg) and integrated this axis into the scanning software. 3D root scans at different soil column depths were realized to fully measure the root architecture, which were concatenated afterwards. Signal to noise ratio allowed the detection of roots with a diameter > ~ 350 µm, which was sufficient to visualize the crown, the seminal and part of the lateral wheat root structure. Digital root fresh weight (DRFW, a.u) was obtained at 7mm-vertical resolution by integrating over each depth interval the intensity of the horizontal MRI signal. The MRI signal intensity, which is proportional to the water content of the roots, was used as proxy of the root biomass. Comparison with the destructive analysis showed (WinRhizo™, see next paragraph), that these roots greater than 350 µm for our wheat lines at the booting stage represented 20% of the total root surface area on average across soil layers. The root angles were obtained by processing the MRI 3D scans with the NMRooting software according to van Dusschoten et al. (2016).

At the end of the experiment (43 DaS), the roots in the acrylic columns were destructively sampled from the soil layers 0–6, 6–17, 17–28, 28–39, 39–50, 50–61, 61–73, 73–80 cm, weighted and scanned (Expression 10000XL Model J181A; EPSON, Japan). The images were analyzed with WinRhizo™ (Regent

Instruments Inc., Quebec, Canada) for determination of the root surface per root diameter classes in each of the aforementioned soil layers. The number of basal roots was assessed by counting them manually on the topsoil root scans and the total root biomass after scanning by drying and weighting them. Aboveground biomass was assessed by sampling the leaves, stems and ears, and drying and weighing them. The water use efficiency (WUE, g/L) was calculated as the ratio of whole plant (above- and below-ground) weight to the amount of cumulated transpired water between the sowing and the booting stage.

2.4 Statistics and data representation

Statistical analyses were performed in R (Version 4.2.0; R Core Team 2020). The qqplot and Levene tests from the car package (Fox et al. 2001) were used to test for normality and homoscedasticity of variance, respectively. When these tests were not positive, the datasets were transformed using the Logarithm or the Squared-Root functions to pass the test of normality. The significance of differences was assessed with a linear mixed-effects model using the lme function from the nlme package (Pinheiro and Bates 2000). Genotype, depth, and water regime were considered as fixed effects, while columns and runs were treated as random effects. We used the following symbols to indicate statistical significance: " ": $p > 0.05$; "*": $p <= 0.05$; "**": $p <= 0.01$; "***": $p <= 0.001$; "****": $p <= 0.0001$. The comparison among treatments were carried out via the emmeans test adjusted with the bonferroni method with the package stat_pwc {ggpubr}. To interpolate the plant aboveground parameter evolution (e.g., leaf number) over the time, the local polynomial regression fitting function "loess" was used.

3 Results

3.1 Root and shoot traits

Across plant modalities and water treatments, the total dry biomass (1.7 ± 0.4 g) and root surface area (32 ± 6 dm^2) was very similar (Table S1). However, the root crown number was significantly higher under WW treatment than under WD (water: $p < 0.001$). Under both WD and WW treatment, the mixture MIX showed on average higher root crown numbers than both monocultures (12% and 15% less respectively under WW; 5% and 15% less under WD; non-significant (NS)) (Table S1). The average root crown angles were similar among the plant modality and the water treatments (Fig. S3).

The digital root fresh weight (DRFW) and the root surface densities were significantly higher in the topsoil than in the other soil layers (depth: $p < 0.001$) (Fig. 2, S4). At shallow depths, both measures of root distribution were greater under the WW treatment than under the WD treatment, and the opposite was observed in subsoil layers (depth x water: $p < 0.001$) (Fig. 2, S4). The DRFW was greater for SRS than for DRS in the topsoil from 0 to 10 cm, whereas DRS showed higher DRFW at soil depths below 40 cm (Fig. 2). The root surface densities generally showed the same patterns in some root diameter classes (Fig. S4). Root distribution across the profile in the MIX treatment was generally between SRS and DRS or on the same level (Fig. 2).

The plant shoot dry biomass at the elongation stage was not significantly different among the treatments and modalities (2.6 ± 1.1 g). Differences between water treatments began to appear on the surface at 35 DaS (stem elongation) and were significant at the booting stage (43 DaS). At this stage, the water deficit treatment significantly decreased the plant shoot surface able to transpire (water: $p < 0.05$) (Fig. 3a-d) and the tiller number per plant became significantly lower for DRS as compared to SRS (plant: $p < 0.05$), which was pronounced for the WD treatment (water x plant: $p < 0.01$) (Fig. 3e-h). However, we noted no significant differences for the leaf stomatal density between the two genotypes (Table S1).

The tiller/crown root ratio, however, was significantly higher under WD than WW (water: $p < 0.01$), and SRS showed higher values than MIX and DRS (plant: $p < 0.05$, Table S1). The biomass and surface area ratios of aboveground and belowground organs remained stable regardless of water treatment and plant modality (resp. 2.92 ± 0.72 and 0.75 ± 0.29).

3.2 Soil water status

With regard to soil water status, the matric potential at the booting stage (between 39 and 42 DaS) was significantly higher in water-deficit (WD) conditions (pF 3.7 ± 0.4 on average) than in well-watered (WW) conditions (pF 2.8 ± 0.6) (water: $p < 0.01$, Fig. 4 and Table 1). The total transpiration throughout the entire experiment (water: $p < 0.05$, Table S1) as well as the hourly transpiration rate between 39 and 43 DaS (water: $p < 0.001$, Fig. S5) were significantly lower under WD. However, the WUE was similar across water treatments and plant modalities (2.38 ± 0.52 $mL.g^{-1}$, Table S1).

The SMP for the different plant modalities showed significant differences at each depth (plant x depth: $p < 0.0001$). In the interactions with water treatment, we observed under WD that SMP profiles all decreased from the topsoil to the subsoil layers for all three plant modalities. However, under optimal WW conditions, the SMP profiles of SRS and DRS were contrasting (Fig. 4). For SRS, SMP profile decreases from dry topsoil (2.62 ± 0.42) to moister subsoil (2.43 ± 0.73). For DRS, the SMP increased from the moist topsoil (2.42 ± 0.35) to the drier subsoil (2.98 ± 0.39), with a local maximum in the middle at 42 cm (3.16 ± 0.34). MIX behaved intermediately, similar to DRS (from moist topsoil to drier subsoil) but with more variability and a shallower local maximum than the DRS one, at 20 cm (3.28 ± 0.49) (Fig. 4).

Thus, this effect of water treatment differed between plant modalities and between profiles, with SRS showing an almost constant difference at all depths, while DRS showed pronounced differences in the upper soil layers and the MIX treatment showed the smallest difference at a depth of 20 cm (plant x water x depth: $p < 0.001$, Fig. 4). When we compared the matric potential “WW-WD” in MPa and not on a logarithmic scale, we found that the largest absolute difference in SMP was in the topsoil and was the most pronounced for SRS (Fig. S6).

3.3 Root water uptake

At the booting stage between 39 and 42 DaS, the wheat roots extracted water more intensively from the topsoil layer (the top 7 cm; 4.04 ± 0.75% cm^{-1} in WW; 4.33 ± 1.4% cm^{-1} in WD), less intensively from subsoil (69 to 80cm; 1.46 ± 0.65% cm^{-1} in WW; 1.96 ± 1.03% cm^{-1} in WD). The least of the fRWU contributions came from intermediate soil layers (0.67 ± 0.34% cm^{-1} WW; 0.57 ± 0.30% cm^{-1} WD) (Fig. 5). However, this pattern changed with the reduction in water availability with the root water uptake intensifying mainly in the subsoil (also to a lesser extent in the topsoil) and decreasing in the intermediate soil layers (depth x water: $p < 0.001$).

The fRWU profiles were also affected by the genotypes with SRS having extracted more water from the topsoil layer than DRS while the opposite was observed in the subsoil layer (depth x plant: $p < 0.001$) (Fig. 5). These differences between DRS and SRS were more prominent for WD compared to WW (water x depth x plant: $p < 0.001$). We observed this same trend within the mixtures under WD, where SRS in mixture (4.23 ± 1.54% cm^{-1}) extracted more water than DRS in mixture in the first 7cm soil layer (3.19 ± 0.87 cm^{-1}) and less in the 76-80cm subsoil layer (2.34 ± 0.35% cm^{-1} SRS in mixture; 3.50 ± 0.54% cm^{-1} DRS in mixture). Thus, under WD we noted a constant absolute difference between DRS and SRS (both in monoculture and mixture) of 1.09 ± 0.46% cm^{-1} from 0 to 7cm and from 76 to 80cm (Fig. 5b).

In a similar vein, it was observed that in mixtures, the absolute root water uptake (Sink Term; mL min^{-1} cm^{-1}) of SRS in the topsoil were higher than those of DRS under WW ($p < 0.001$) (Fig. 6a). Under WD, the SRS also absorbed more water than the DRS between 0 and 2 cm ($p < 0.05$), but in the subsoil DRS absorbed much more water than SRS ($p < 0.001$) (Fig. 6b). However, in monoculture under WW, DRS transpired significantly more than SRS (Fig. S5) and differences appeared in the topsoil ($p < 0.05$) (Fig. 6c) while under WD, with more equivalent transpiration, DRS absorbed more water than SRS in the subsoil ($p < 0.05$) (Fig. 6d). In addition to this relative difference between SRS and DRS, it was found that both genotypes in mixture under WD reduced their water extraction from the topsoil compared to monoculture (-1.2% cm^{-1} on average for layers 0 to 7 cm; at these depths, water x plant: $p < 0.001$). In contrast, both increased their fRWU from the subsoil layers in mixture (+ 0.5% cm^{-1} for layers 69 to 80 cm; at these depths, water x plant: $p < 0.001$) (Fig. 5b). However, this was reversed under WW, with both SRS and DRS in mixture extracting more water from the surface than the same genotypes in monoculture (+ 2.0% cm^{-1} from 2 to 7 cm depth) (Fig. 5a).

The amplitude of root water uptake plasticity in response to water deficit differed for each plant modality (Fig. 7). By calculating the difference between the fRWU profiles under WD and those under WW, it can be observed that SRS exhibited a significantly higher level of contribution in the initial 30 centimeters of soil in order to cope with water deficiency. This result was less pronounced for DRS in subsoil, but it greatly increased the amplitude of the fRWU's shift toward subsoil (i.e., its "natural niche") in response to water deficit. In the context of mixture, both DRS and SRS exhibited comparable WW-WD plasticity profiles for fRWU, which resulted in a decrease in their contribution in the topsoil and an increase in the subsoil. However, this effect was more pronounced for DRS than for SRS (Fig. 7).

When the vertical distribution of fRWU (% cm-1) and root biomass density (dDRFW, % cm-1) were compared layer by layer, it was observed that most points were proportional (Fig. 8). The mixed linear regression of dDRFW explaining fRWU, taking into account the random effect of depths, shows a conditional R^2 of 0.67. Two main areas were identified where biomass and water uptake values were found to be non-proportional. Firstly, in the topsoil (0–4 cm), root biomass densities were found to be almost twice as high as their respective water uptake fractions. Secondly, in the subsoil, between 76 and 78 cm deep, the fRWUs were much higher than their corresponding root biomasses. Furthermore, it was observed that for the SRS under WD at 4–7 cm, the fRWUs exhibited higher values in comparison to the dDRFWs (Fig. 8).

4 Discussion

4.1 Root architectures and water uptake

In the present study, the first hypothesis was corroborated, namely that the SRS genotype in monoculture extracts more water in the topsoil layers than the DRS genotype in monoculture, and the converse is observed in the subsoil layers, especially under chronical water deficit conditions (Fig. 5, 6, 7). These contrasts between the genotype fRWU may have occurred not only at the booting stage, but also already at earlier development stages, as aboveground plant traits began to be affected by chronic water treatment starting from stem elongation (Fig. 3). Evidence was provided by the soil pF profiles at this booting stage, which exhibited significant differences between the genotypes, reflecting contrasted root water uptake histories in the soil columns in both water treatments (Fig. 4). Previous studies have explained that discrepancies in root water uptake through soil profiles can be partially attributed to variations in root biomass distribution (Fort et al. 2017; McMurtrie et al. 2012). This was also the case in our study with the distribution of MRI assessed root biomass exhibited higher values in the topsoil for SRS and in the subsoil for DRS (NS; Fig. 2) and that this root biomass density profile (dDRFW, % cm^{-1}) could explain 67% of the fRWU (% cm^{-1}) distribution variability for both genotypes in monoculture (Fig. 8). However, a diminished water uptake per root biomass was also evident in the topsoil, while an increase was observed in the subsoil (Fig. 8). Physiological processes such as suberization, cambial growth, tissue maturation, and the loss of the root hair system, particularly in cases of stress (Freschet et al. 2021; Kreszies et al. 2019; Schneider et al. 2020; White and Kirkegaard 2010) could have affected the root water uptake properties in the topsoil.

Besides the root biomass, the fine root distribution plays an important role for the activity of the roots (Bramley et al. 2009; Fort et al. 2017). Indeed, we observed that fine roots were more abundant in the topsoil for SRS, while comparatively higher levels were found in the subsoil for DRS (Fig. S4). Lattacher et al. (2025b) also observed in the same experiment, following a ^{13}C-CO_2 labelling, an increased $\delta^{13}C$ signal in the subsoil roots for MIX and DRS compared to SRS in both water treatments, thus confirming contrasted root activities for these plant modalities.

It is noteworthy that, while the disparity in basal root angles between the two genotypes – the initial selection criterion – proved significant in the early stages of development (Rambla et al. 2022), in our experiment at booting stage these differences were only marginal and no longer significant (Fig. S3). This highlights the fact that the early characterization of root architectures is not necessarily a good indicator for later stages. Therefore, it is imperative to validate these root architectures results at the different studied stages of development (Comas et al. 2013).

4.2 Genotypes strategies facing water deficit

In the present study, the root water uptake strategy facing water deficit consisted of maintaining the important topsoil root water uptake contribution, while also increasing subsoil layer water uptake contributions - in particular by increasing their root biomasses at these soil layers (Fig. 2). This strategy was more pronounced for DRS than SRS in monoculture (Fig. 7). This finding aligned with the extant literature, which also indicated that grassland species facing a water deficit showed a preference for maintaining root water uptake from the topsoil, despite lower soil water availability (Deseano Diaz et al. 2023; Prechsl et al. 2015). In a separate study on another drought-exposed *Poaceae* species (Giant reed), it was observed that while a substantial increase in water uptake was recorded in the subsoil layers, an enhancement in the efficiency of water uptake by surface roots was concurrently evident (Zegada-Lizarazu and Monti 2019). This finding provides partial validation for the second hypothesis, which postulated that the distribution of root water uptake intensity is influenced by the soil matric potential, as root water uptake profiles notably differed according to the water treatment (Fig. 7). However, the hypothesized strong fRWU shift toward wetter subsoil layers under water deficit has not been observed. The observed discrepancies between SMP (Fig. 4) and fRWU (Fig. 5) profiles demonstrate that root water uptake is not solely dependent on soil water availability, but also on other factors, such as the hydraulic conductance of the root system (Krs) (Delval et al. 2024; Müllers et al. 2023; Rickard et al. 2025).

Beyond the similarities in response to water deficit between the two wheat genotypes, it was observed that the surface area of fine roots (less than 250 µm) in contact with the soil was significantly greater for SRS than for DRS in the topsoil (Fig. S4). This difference under water deficit may have resulted, for SRS, in better root hydraulic conductance and greater root exudation in this soil layer, enhancing the soil's hydro-physical properties in the rhizosphere (Bramley et al. 2009; Doussan et al. 2024; Le Gall et al. 2024; McDougall and Rovira 1970). Thus, in the topsoil above 7 cm under water-deficit conditions, although the measured MRI root biomasses were similar, the relative contributions of root water uptake were higher for SRS than for DRS (Fig. 8). The observed fRWU patterns differences among the plant modalities facing water deficit could also be due to the presence of arbuscular mycorrhizal fungi (AMF), which have been shown to be associated with the roots uptake dynamics (Zaman et al. 2024). Indeed, under WD, AMF have been found to be more prevalent in the topsoil of SRS monoculture, and conversely in the deeper soil layers for DRS monoculture (Lattacher et al. 2025b).

From a physiological perspective, it was observed that DRS exhibited greater sensitivity to water deficit compared to SRS, as evidenced by the reduction in the number of tillers and total leaf area from 35 days

after sowing, i.e., nearly a week before the booting stage studied (Fig. 3). Moreover, no substantial differences were noted between the two genotypes with respect to leaf stomatal density or crown root number (Table S1), which might have partially account for the observed discrepancy in terms of water deficit tolerance. These observations demonstrate that greater deep root water uptake does not necessarily result in lower sensitivity to water deficit, as it has been observed in other studies, even when water is available at depth (Sun et al. 2011). Indeed, the impact of root architectures on adaptation to water deficit depends on the growth stage and the intensity of the drought (Comas et al. 2013; Tardieu 2012). In our case, the deep-rooted DRS genotype may have incurred a higher metabolic cost and a greater investment in photoassimilates than SRS to maintain deep root activity, leading to reduced shoot growth or limited stomatal regulation in response to prolonged water deficit (Li et al. 2022; Tardieu 2012).

4.3 A niche complementarity in the wheat genotype mixture?

In the mixture, the two genotypes exhibited distinct fRWU profiles corresponding to their respective preferred niches, a particularly significant characteristic under water-deficient conditions (Figs. 5 and 7). Lattacher et al. (2025b) used an independent method involving 15N labeling to demonstrate that the SRS genotype in monoculture extracted more nitrogen (enabled by the root water uptake, which contains nutrients) from the topsoil than the DRS, with a more pronounced effect in mixtures under water deficit conditions (Gorska et al. 2008; Plett et al. 2020). These observations support the hypothesis that minor variations in root biomass distribution between two root systems developed in the same soil profile (Fig. 2) can significantly impact water uptake patterns (Kulmatiski et al. 2020).

The maintenance or even increase of these contrasting patterns of nutrient and water uptake by genotypes has been shown to allow for a better spatial distribution of access to these resources in the event of water deficit in mixtures (Vidal et al. 2020; Kong et al. 2023; Stefan et al. 2025). This phenomenon may partly explain the high or higher yield and better protein quality under these conditions.

The third hypothesis of our study focused on the conservation of contrasted root water uptake distribution of the two genotypes in the mixture, allowing for “hydrological niche segregation” (Zhao et al., 2024). In the mixture, the two genotypes exhibited distinct fRWU profiles corresponding to their respective preferred niches, a particularly significant characteristic under water-deficient conditions (Figs. 5 and 7). Lattacher et al. (2025b) used an independent method involving 15N labeling to demonstrate that the SRS genotype in monoculture extracted more nitrogen (enabled by the root water uptake, which contains nutrients) from the topsoil than the DRS, with a more pronounced effect in mixtures under water deficit conditions (Gorska et al. 2008; Plett et al. 2020). These observations supports the view that slight variations in root biomass distribution between two root systems developed in the same soil profile (Fig. 2) can have a significant impact on water uptake patterns (Kulmatiski et al. 2020). The maintenance, or even increase, of these contrasting nutrient and water

uptake patterns by the genotypes allowed better spatial distribution of access to these resources under water deficit in the mixtures, which can partly explain the high or higher yield and protein quality in such condition (Vidal et al. 2020; Kong et al. 2023; Stefan et al. 2025).

Furthermore, it was observed that, in addition to niche complementarity in terms of access to water and nutrients between the two fRWU strategies compared to monoculture, the mixture of SRS and DRS led to a systematic increase in fRWU towards the subsoil layers and a decrease in the topsoil layer in situations of water deficit (Figs. 5 and 7). Beside, a significantly higher number of seminal roots was observed in the mixture compared to the two monocultures, regardless of water treatment, despite similar root biomass (Table 2). The high number of crown roots has been associated with an increase in topsoil foraging, as indicated by Lynch (2022). This observation suggests that, initial stronger competition between the two genotypes in the mixture for access to topsoil resources may force them to increase contributions from deeper layers at the booting stage. This dynamic of increased water uptake in the subsoil has also been observed in various associated species of grassland plants, mixed forest trees, and crop, and was attributed to stronger competition in the topsoil layer (Demir et al. 2024; Guderle et al. 2018; Schmutz and Schöb 2023). Notably, this is the first documented instance of this phenomenon being observed among genotypes of the same species, specifically *Triticum aestivum L.* The plasticity of root water uptake pattern is thus not solely determined by genotype root architecture and soil water availability traits (Fromm 2019), but also by the interaction with the root architectures of the neighboring plant, i.e. in this case the wheat cropping practice in mixture or monoculture.

5 Conclusion

This study demonstrates that mixing wheat genotypes with contrasting root architectures (deep- and shallow-rooted) leads to complementary root water uptake strategies, particularly under water deficit. Using stable isotope tracing (δ^2H and $\delta^{18}O$) and high-resolution root imaging, we quantified distinct vertical RWU patterns: the shallow-rooted genotype (SRS) absorbed significantly more water from the top 7cm of soil, while the deep-rooted genotype (DRS) showed greater uptake in deeper layers (69–80 cm), especially when water was limited.

In mixtures, these uptake patterns were preserved, with RWU shifting toward deeper layers under drought —by approximately 0.5% cm^{-1}—while decreasing in the topsoil. The number of crown roots was also higher in mixtures compared to monocultures, suggesting enhanced soil exploration despite similar total root biomass. To our knowledge, this is the first time that single species hydrological niche separation is demonstrated. Furthermore, these findings suggest that contrasting wheat root architecture mixture may enhance root water uptake complementarity during periods of water deficit at this critical growth stage, which could potentially lead to an increase in yield.

This study highlights how fine-scale monitoring of root water uptake can reveal the benefits of intra-specific diversity for improving water use in cropping systems. However, it also demonstrates that high-resolution root architectural data alone are insufficient to predict RWU distribution under heterogeneous

matric potential conditions, emphasizing the need for direct or indirect RWU measurements through, for instance, stable isotope labelling experiments. However, the effect of water deficit on intraspecific root interaction during plant diurnal cycles, which allows potential hydraulic lifting to be observed, remains to be studied. Finally, the results of this study support the strategic design of genotype mixtures as a practical approach to enhance resilience to drought, offering potential benefits for yield stability and resource efficiency under climate change conditions.

Declarations

Conflicts of interest/Competing interests

The authors have no relevant financial or non-financial interests to disclose.

Funding

The authors acknowledge funding by the German Federal Ministry of Education and Research (BMBF) in the framework of the funding measure "Plant roots and soil ecosystems, significance of the rhizosphere for the bioeconomy" (Rhizo4Bio), subproject CROP phase (FKZ 031B0909). Holger Pagel appreciates funding from the German Research Foundation (DFG) under Germany's Excellence Strategy (EXC 2070 – 1200 390732324). The experimental wheat genotypes examined in this study were developed through the Grains Research and Development Corporation (GRDC) "Rooty" project (ID 9176855), which formed part of the International Wheat Yield Partnership Consortium (IWYP122).

Authors' contributions

Samuel Le Gall, Adrian Lattacher, Mona Giraud, Holger Pagel, Andrea Schnepf, Guillaume Lobet, Ellen Kandeler, Christian Poll, Mathieu Javaux and Youri Rothfuss developed the study concept. Samuel Le Gall, Dagmar van Dusschoten, Adrian Lattacher, Mona Giraud, Moritz Harings, Paulina Deseano Diaz, Guillaume Lobet, Christian Poll, Mathieu Javaux and Youri Rothfuss contributed to build the experimental design and conduct the study. Samir Alahmad and Lee Hickey developed and provided the required wheat genotypes. Samuel Le Gall and Moritz Harings constructed, automated and adjusted the entire experimental platform, according to the recommendations of Paulina Deseano Diaz, Dagmar van Dusschoten and Youri Rothfuss. Samuel Le Gall, Dagmar van Dusschoten, Adrian Lattacher, Mona Giraud, Moritz Harings, Ahmet Sircan and Youri Rothfuss conducted the column experiment in the climate chamber and collected the data. Daniel Pflugfelder and Dagmar van Dusschoten assisted Samuel Le Gall in performing and analyzing the MRI scans. Samuel Le Gall analyzed the samples, evaluated the data and performed statistics with the contribution of Christian Poll, Mathieu Javaux and Youri Rothfuss. Samuel Le Gall wrote the first draft of the manuscript under the supervision of Mathieu Javaux and Youri Rothfuss. All authors critically revised previous versions of the manuscript.

Acknowledgments

The authors would like to thank Johannes Kochs for his strong technical support, Nicolas Brüggemann and Nikolaos Kaloterakis for sharing their controlled condition experiment knowledge, Sirgit Kümmer and Holger Wissel for their support with the isotopic analyses, Franz Leitner for his technical support and Normen Hermes for his help with the LabView programming. We gladly acknowledge the help of Fabian Isensee and Lars Krämer from the Helmholtz imaging support hub who developed the MRI root segmentation neural network. Akhil Brijesh, Sandisiwe Moyo, Christoph Tempelmann, Esther Vogt, Humza Muhammad, Anna Hollweg and Chao Gao provided technical assistance to allow the execution of the experiments and the subsequent analysis of the resulting data. The authors would also like to thank Molly Gilbertson for English corrections.

Data availability

The datasets generated during this study are available from the corresponding author on request

Code availability

This is not applicable to the manuscript.

References

1. Albert CH, Grassein F, Schurr FM et al (2011) When and how should intraspecific variability be considered in trait-based plant ecology? Perspect Plant Ecol Evol Syst 13:217–225. https://doi.org/10.1016/j.ppees.2011.04.003
2. Altieri MA, Nicholls CI, Montalba R (2017) Technological Approaches to Sustainable Agriculture at a Crossroads: An Agroecological Perspective. Sustainability 9:349. https://doi.org/10.3390/su9030349
3. Barot S, Allard V, Cantarel A et al (2017) Designing mixtures of varieties for multifunctional agriculture with the help of ecology. A review. Agron Sustain Dev 37:13. https://doi.org/10.1007/s13593-017-0418-x
4. Blanc L, Lampurlanés J, Simon-Miquel G et al (2024) Rapeseed-pea intercrop outperforms wheat-legume ones in land-use efficiency in Mediterranean conditions. Field Crops Res 318:109612. https://doi.org/10.1016/j.fcr.2024.109612
5. Borg J, Kiær LP, Lecarpentier C et al (2018) Unfolding the potential of wheat cultivar mixtures: A meta-analysis perspective and identification of knowledge gaps. Field Crops Res 221:298–313. https://doi.org/10.1016/j.fcr.2017.09.006
6. Bramley H, Turner NC, Turner DW, Tyerman SD (2009) Roles of Morphology, Anatomy, and Aquaporins in Determining Contrasting Hydraulic Behavior of Roots. Plant Physiol 150:348–364.

https://doi.org/10.1104/pp.108.134098

7. Brannan T, Bickler C, Hansson H et al (2023) Overcoming barriers to crop diversification uptake in Europe: A mini review. Front Sustain Food Syst 7
8. Brooker RW, Bennett AE, Cong W-F et al (2015) Improving intercropping: a synthesis of research in agronomy, plant physiology and ecology. New Phytol 206:107–117. https://doi.org/10.1111/nph.13132
9. Bruelheide H, Dengler J, Purschke O et al (2018) Global trait–environment relationships of plant communities. Nat Ecol Evol 2:1906–1917. https://doi.org/10.1038/s41559-018-0699-8
10. Bybee-Finley KA, Ryan MR (2018) Advancing Intercropping Research and Practices in Industrialized Agricultural Landscapes. Agriculture 8:80. https://doi.org/10.3390/agriculture8060080
11. Chabert S, Eeraerts M, DeVetter LW et al (2024) Intraspecific crop diversity for enhanced crop pollination success. A review. Agron Sustain Dev 44:50. https://doi.org/10.1007/s13593-024-00984-2
12. Chanda SV, Singh YD (2002) Estimation of leaf area in wheat using linear measurements. Plant Breed Seed Sci 46:75–79
13. Comas L, Becker S, Cruz VMV et al (2013) Root architectures contributing to plant productivity under drought. Front Plant Sci 4. https://doi.org/10.3389/fpls.2013.00442
14. Couvreur V, Rothfuss Y, Meunier F et al (2020) Disentangling temporal and population variability in plant root water uptake from stable isotopic analysis: when rooting depth matters in labeling studies. Hydrol Earth Syst Sci 24:3057–3075. https://doi.org/10.5194/hess-24-3057-2020
15. Cowger C, Mundt CC (2002) Effects of Wheat Cultivar Mixtures on Epidemic Progression of Septoria Tritici Blotch and Pathogenicity of Mycosphaerella graminicola. Phytopathology® 92:617–623. https://doi.org/10.1094/PHYTO.2002.92.6.617
16. Delval L, Vanderborght J, Javaux M (2024) Combination of plant and soil water potential monitoring and modelling demonstrates soil-root hydraulic disconnection during drought. Plant Soil. https://doi.org/10.1007/s11104-024-07062-2
17. Demie DT, Döring TF, Finckh MR et al (2022) Mixture × Genotype Effects in Cereal/Legume Intercropping. Front Plant Sci 13:846720. https://doi.org/10.3389/fpls.2022.846720
18. Demir G, Guswa AJ, Filipzik J et al (2024) Root water uptake patterns are controlled by tree species interactions and soil water variability. Hydrol Earth Syst Sci 28:1441–1461. https://doi.org/10.5194/hess-28-1441-2024
19. Deseano Diaz PA, van Dusschoten D, Kübert A et al (2023) Response of a grassland species to dry environmental conditions from water stable isotopic monitoring: no evident shift in root water uptake to wetter soil layers. Plant Soil 482:491–512. https://doi.org/10.1007/s11104-022-05703-y
20. Doussan C, Gall SL, Ruy S, Bérard A (2024) Utiliser les racines pour moduler les impacts des déficits en eau et améliorer la gestion de l'eau dans les agrosystèmes. Sci Eaux Territ 8144–8144. https://doi.org/10.20870/Revue-SET.2024.45.8144

21. Dubin HJ, Wolfe MS (1994) Comparative behavior of three wheat cultivars and their mixture in India, Nepal and Pakistan. Field Crops Res 39:71–83. https://doi.org/10.1016/0378-4290(94)90010-8
22. Duchene O, Celette F, Barreiro A et al (2020) Introducing Perennial Grain in Grain Crops Rotation: The Role of Rooting Pattern in Soil Quality Management. Agronomy 10:1254. https://doi.org/10.3390/agronomy10091254
23. Duchene O, Vian J-F, Celette F (2017) Intercropping with legume for agroecological cropping systems: Complementarity and facilitation processes and the importance of soil microorganisms. A review. Agric Ecosyst Environ 240:148–161. https://doi.org/10.1016/j.agee.2017.02.019
24. El Hassouni K, Alahmad S, Belkadi B et al (2018) Root System Architecture and Its Association with Yield under Different Water Regimes in Durum Wheat. Crop Sci 58:2331–2346. https://doi.org/10.2135/cropsci2018.01.0076
25. Feng S, Gu S, Zhang H, Wang D (2017) Root vertical distribution is important to improve water use efficiency and grain yield of wheat. Field Crops Res 214:131–141. https://doi.org/10.1016/j.fcr.2017.08.007
26. Fischer RA (1985) Number of kernels in wheat crops and the influence of solar radiation and temperature. J Agric Sci 105:447–461. https://doi.org/10.1017/S0021859600056495
27. Fort F, Volaire F, Guilioni L et al (2017) Root traits are related to plant water-use among rangeland Mediterranean species. Funct Ecol 31:1700–1709. https://doi.org/10.1111/1365-2435.12888
28. Fox J, Weisberg S, Price B (2001) car: Companion to Applied Regression. 3.1-3
29. Francesco Giovanni Salvo A, Mariotti M, Tozzi B et al (2022) Herbage and silage quality improved more by mixing hybrid barley and faba bean than by N fertilization or stage of harvest. https://doi.org/10.3390/agronomy12081790. Agronomy
30. Freschet GT, Pagès L, Iversen CM et al (2021) A starting guide to root ecology: strengthening ecological concepts and standardising root classification, sampling, processing and trait measurements. New Phytol 232:973–1122. https://doi.org/10.1111/nph.17572
31. Fromm H (2019) Root Plasticity in the Pursuit of Water. Plants 8:236. https://doi.org/10.3390/plants8070236
32. Gaba S, Lescourret F, Boudsocq S et al (2015) Multiple cropping systems as drivers for providing multiple ecosystem services: from concepts to design. Agron Sustain Dev 35:607–623. https://doi.org/10.1007/s13593-014-0272-z
33. Giraud M, Gall SL, Harings M et al (2023) CPlantBox: a fully coupled modelling platform for the water and carbon fluxes in the soil–plant–atmosphere continuum. Silico Plants 5:diad009. https://doi.org/10.1093/insilicoplants/diad009
34. Gorska A, Ye Q, Holbrook NM, Zwieniecki MA (2008) Nitrate control of root hydraulic properties in plants: translating local information to whole plant response. Plant Physiol 148:1159–1167. https://doi.org/10.1104/pp.108.122499
35. Guderle M, Bachmann D, Milcu A et al (2018) Dynamic niche partitioning in root water uptake facilitates efficient water use in more diverse grassland plant communities. Funct Ecol 32:214–227.

https://doi.org/10.1111/1365-2435.12948

36. Hafeez A, Ali S, Javed MA et al (2024) Breeding for water-use efficiency in wheat: progress, challenges and prospects. Mol Biol Rep 51:429. https://doi.org/10.1007/s11033-024-09345-4
37. Hawes C, Iannetta PPM, Squire GR (2021) Agroecological practices for whole-system sustainability. https://doi.org/10.1079/PAVSNNR202116005. CABI Rev 2021:
38. Homulle Z, George TS, Karley AJ (2022) Root traits with team benefits: understanding belowground interactions in intercropping systems. Plant Soil 471:1–26. https://doi.org/10.1007/s11104-021-05165-8
39. Hughes AR, Inouye BD, Johnson MTJ et al (2008) Ecological consequences of genetic diversity. Ecol Lett 11:609–623. https://doi.org/10.1111/j.1461-0248.2008.01179.x
40. Jung V, Violle C, Mondy C et al (2010) Intraspecific variability and trait-based community assembly. J Ecol 98:1134–1140. https://doi.org/10.1111/j.1365-2745.2010.01687.x
41. Kong X, Li L, Peng P et al (2023) Wheat cultivar mixtures increase grain yield under varied climate conditions. Basic Appl Ecol 69:13–25. https://doi.org/10.1016/j.baae.2023.03.007
42. Kreszies T, Shellakkutti N, Osthoff A et al (2019) Osmotic stress enhances suberization of apoplastic barriers in barley seminal roots: analysis of chemical, transcriptomic and physiological responses. New Phytol 221:180–194. https://doi.org/10.1111/nph.15351
43. Kühnhammer K, Kübert A, Brüggemann N et al (2020) Investigating the root plasticity response of Centaurea jacea to soil water availability changes from isotopic analysis. New Phytol 226:98–110. https://doi.org/10.1111/nph.16352
44. Kulmatiski A, Beard KH, Holdrege MC, February EC (2020) Small differences in root distributions allow resource niche partitioning. Ecol Evol 10:9776–9787. https://doi.org/10.1002/ece3.6612
45. Lamichhane JR, Arseniuk E, Boonekamp P et al (2018) Advocating a need for suitable breeding approaches to boost integrated pest management: a European perspective. Pest Manag Sci 74:1219–1227. https://doi.org/10.1002/ps.4818
46. Lattacher A, Le Gall S, Rothfuss Y et al (2025a) Rooting for microbes: impact of root architecture on the microbial community and function in top- and subsoil. Plant Soil. https://doi.org/10.1007/s11104-024-07181-w
47. Lattacher A, Le Gall S, Rothfuss Y et al (2025b) Combining root-contrasted phenotypes of spring wheat modifies plant-microbe interactions under different water regimes. Submitt, Plant Soil
48. Le Gall S, Lapie C, Cajot F et al (2024) Chemical diversity of crop root mucilages: Implications for their maximal water content and decomposition. Rhizosphere 29:100858. https://doi.org/10.1016/j.rhisph.2024.100858
49. Lecarpentier C, Barillot R, Blanc E et al (2019) WALTer: a three-dimensional wheat model to study competition for light through the prediction of tillering dynamics. Ann Bot 123:961–975. https://doi.org/10.1093/aob/mcy226

50. Li B, Zhang X, Morita S et al (2022) Are crop deep roots always beneficial for combating drought: A review of root structure and function, regulation and phenotyping. Agric Water Manag 271:107781. https://doi.org/10.1016/j.agwat.2022.107781
51. Li L, Giller P, Peng P et al (2023) The genetic diversity-productivity effect in wheat cultivar mixtures at multiple levels. Eur J Agron 142:126676. https://doi.org/10.1016/j.eja.2022.126676
52. Litrico I, Violle C (2015) Diversity in Plant Breeding: A New Conceptual Framework. Trends Plant Sci 20:604–613. https://doi.org/10.1016/j.tplants.2015.07.007
53. Lynch JP (2022) Harnessing root architecture to address global challenges. Plant J 109:415–431. https://doi.org/10.1111/tpj.15560
54. McAlvay AC, DiPaola A, D'Andrea AC et al (2022) Cereal species mixtures: an ancient practice with potential for climate resilience. A review. Agron Sustain Dev 42:100. https://doi.org/10.1007/s13593-022-00832-1
55. McDougall BM, Rovira AD (1970) Sites of Exudation of 14c-Labelled Compounds from Wheat Roots. New Phytol 69:999–1003. https://doi.org/10.1111/j.1469-8137.1970.tb02479.x
56. McMurtrie RE, Iversen CM, Dewar RC et al (2012) Plant root distributions and nitrogen uptake predicted by a hypothesis of optimal root foraging. Ecol Evol 2:1235–1250. https://doi.org/10.1002/ece3.266
57. Messéan A, Viguier L, Paresys L, ENABLING CROP DIVERSIFICATION TO SUPPORT TRANSITIONS TOWARD MORE SUSTAINABLE EUROPEAN AGRIFOOD SYSTEMS (2021) Front Agric Sci Eng 8:474–480. https://doi.org/10.15302/J-FASE-2021406
58. Mettauer R, Thoumazeau A, Le Gall S et al (2023) Soil health in temperate agroforestry: influence of tree species and position in the field. Arch Agron Soil Sci 69:1781–1800. https://doi.org/10.1080/03650340.2022.2116013
59. Mille B, Fraj MB, Monod H, de Vallavieille-Pope C (2006) Assessing Four-Way Mixtures of Winter Wheat Cultivars from the Performances of their Two-Way and Individual Components. Eur J Plant Pathol 114:163–173. https://doi.org/10.1007/s10658-005-4036-0
60. Moreau P, Ruiz L, Raimbault T et al (2012) Modeling the potential benefits of catch-crop introduction in fodder crop rotations in a Western Europe landscape. Sci Total Environ 437:276–284. https://doi.org/10.1016/j.scitotenv.2012.07.091
61. Müllers Y, Postma JA, Poorter H, van Dusschoten D (2023) Deep-water uptake under drought improved due to locally increased root conductivity in maize, but not in faba bean. Plant Cell Environ 46:2046–2060. https://doi.org/10.1111/pce.14587
62. Mundt CC (2002) Use of multiline cultivars and cultivar mixture for disease management. Annu Rev Phytopathol 40:381–410. https://doi.org/10.1146/annurev.phyto.40.011402.113723
63. Nakhforoosh A, Grausgruber H, Kaul H-P, Bodner G (2014) Wheat root diversity and root functional characterization. Plant Soil 380:211–229. https://doi.org/10.1007/s11104-014-2082-0
64. Nerlich K, Graeff-Hönninger S, Claupein W (2013) Agroforestry in Europe: a review of the disappearance of traditional systems and development of modern agroforestry practices, with

emphasis on experiences in Germany. Agrofor Syst 87:475–492. https://doi.org/10.1007/s10457-012-9560-2

65. Newton AC, Swanston JS, Guy DC, Ellis RP (1998) The Effect of Cultivar Mixtures on Malting Quality in Winter Barley. J Inst Brew 104:41–45. https://doi.org/10.1002/j.2050-0416.1998.tb00973.x
66. Ortiz R, Sayre KD, Govaerts B et al (2008) Climate change: Can wheat beat the heat? Agric Ecosyst Environ 126:46–58. https://doi.org/10.1016/j.agee.2008.01.019
67. Parnell AC, Inger R, Bearhop S, Jackson AL (2010) Source Partitioning Using Stable Isotopes: Coping with Too Much Variation. PLoS ONE 5:e9672. https://doi.org/10.1371/journal.pone.0009672
68. Pathoumthong P, Zhang Z, Roy SJ, El Habti A (2023) Rapid non-destructive method to phenotype stomatal traits. Plant Methods 19:36. https://doi.org/10.1186/s13007-023-01016-y
69. Perrone R, Rolland B, Mabire C et al (2017) Evolution of adoption of variety mixtures and low-input multi-resistant bread wheat varieties since two decades in France. IDEEV Day Gif-Sur-Yvette
70. Pinheiro JC, Bates DM (eds) (2000) Linear Mixed-Effects Models: Basic Concepts and Examples. Mixed-Effects Models in S and S-PLUS. Springer, New York, NY, pp 3–56
71. Plett DC, Ranathunge K, Melino VJ et al (2020) The intersection of nitrogen nutrition and water use in plants: new paths toward improved crop productivity. J Exp Bot 71:4452–4468. https://doi.org/10.1093/jxb/eraa049
72. Prechsl UE, Burri S, Gilgen AK et al (2015) No shift to a deeper water uptake depth in response to summer drought of two lowland and sub-alpine C3-grasslands in Switzerland. Oecologia 177:97–111. https://doi.org/10.1007/s00442-014-3092-6
73. Rambla C, Van Der Meer S, Voss-Fels KP et al (2022) A toolkit to rapidly modify root systems through single plant selection. Plant Methods 18:2. https://doi.org/10.1186/s13007-021-00834-2
74. Rickard W, Hossain I, Zhang X et al (2025) Field plants strategically regulate water uptake from different soil depths by spatiotemporally adjusting their radial root hydraulic conductivity. New Phytol n/a: https://doi.org/10.1111/nph.70013
75. Rothfuss Y, Vereecken H, Brüggemann N (2013) Monitoring water stable isotopic composition in soils using gas-permeable tubing and infrared laser absorption spectroscopy. Water Resour Res 49:3747–3755. https://doi.org/10.1002/wrcr.20311
76. Schmutz A, Schöb C (2023) Crops grown in mixtures show niche partitioning in spatial water uptake. J Ecol 111:1151–1165. https://doi.org/10.1111/1365-2745.14088
77. Schneider HM, Postma JA, Kochs J et al (2020) Spatio-Temporal Variation in Water Uptake in Seminal and Nodal Root Systems of Barley Plants Grown in Soil. Front Plant Sci 11. https://doi.org/10.3389/fpls.2020.01247
78. Schöb C, Engbersen N, López-Angulo J et al (2023) Crop Diversity Experiment: towards a mechanistic understanding of the benefits of species diversity in annual crop systems. J Plant Ecol. https://doi.org/10.1093/jpe/rtad016. rtad016

79. Sharma RC, Dubin HJ (1996) Effect of wheat cultivar mixtures on spot blotch (Bipolaris sorokiniana) and grain yield. Field Crops Res 48:95–101. https://doi.org/10.1016/S0378-4290(96)01031-3
80. Shazadi K, Christopher JT, Chenu K (2024) Does late water deficit induce root growth or senescence in wheat? Front Plant Sci 15. https://doi.org/10.3389/fpls.2024.1351436
81. Stefan L, Strebel S, Camp K-H et al (2025) Multi-trait assessment of wheat variety mixtures performance and stability: Mixtures for the win! Eur J Agron 164:127504. https://doi.org/10.1016/j.eja.2024.127504
82. Sun S-J, Meng P, Zhang J-S, Wan X (2011) Variation in soil water uptake and its effect on plant water status in Juglans regia L. during dry and wet seasons. Tree Physiol 31:1378–1389. https://doi.org/10.1093/treephys/tpr116
83. Tardieu F (2012) Any trait or trait-related allele can confer drought tolerance: just design the right drought scenario. J Exp Bot 63:25–31. https://doi.org/10.1093/jxb/err269
84. van Dusschoten D, Metzner R, Kochs J et al (2016) Quantitative 3D Analysis of Plant Roots Growing in Soil Using Magnetic Resonance Imaging. Plant Physiol 170:1176–1188. https://doi.org/10.1104/pp.15.01388
85. Vanneste T, Govaert S, De Kesel W et al (2020) Plant diversity in hedgerows and road verges across Europe. J Appl Ecol 57:1244–1257. https://doi.org/10.1111/1365-2664.13620
86. Vidal T, Saint-Jean S, Lusley P et al (2020) Cultivar mixture effects on disease and yield remain despite diversity in wheat height and earliness. Plant Pathol 69:1148–1160. https://doi.org/10.1111/ppa.13200
87. Vincent-Caboud L, Casagrande M, David C et al (2019) Using mulch from cover crops to facilitate organic no-till soybean and maize production. A review. Agron Sustain Dev 39:45. https://doi.org/10.1007/s13593-019-0590-2
88. Wang Z, Zhang B, Li J et al (2024) Effects of Deficit-Regulated Irrigation on Root-Growth Dynamics and Water-Use Efficiency of Winter Wheat in a Semi-Arid Area. Water 16:2678. https://doi.org/10.3390/w16182678
89. Wasson AP, Richards RA, Chatrath R et al (2012) Traits and selection strategies to improve root systems and water uptake in water-limited wheat crops. J Exp Bot 63:3485–3498. https://doi.org/10.1093/jxb/ers111
90. Weihermüller L, Huisman JA, Lambot S et al (2007) Mapping the spatial variation of soil water content at the field scale with different ground penetrating radar techniques. J Hydrol 340:205–216. https://doi.org/10.1016/j.jhydrol.2007.04.013
91. Wezel A, Casagrande M, Celette F et al (2014) Agroecological practices for sustainable agriculture. A review. Agron Sustain Dev 34:1–20. https://doi.org/10.1007/s13593-013-0180-7
92. White RG, Kirkegaard JA (2010) The distribution and abundance of wheat roots in a dense, structured subsoil – implications for water uptake. Plant Cell Environ 33:133–148. https://doi.org/10.1111/j.1365-3040.2009.02059.x

93. Wilcox J, Makowski D (2014) A meta-analysis of the predicted effects of climate change on wheat yields using simulation studies. Field Crops Res 156:180–190. https://doi.org/10.1016/j.fcr.2013.11.008
94. Wu W, Wang Y, Wang L et al (2022) Booting stage is the key timing for split nitrogen application in improving grain yield and quality of wheat – A global meta-analysis. Field Crops Res 287:108665. https://doi.org/10.1016/j.fcr.2022.108665
95. Xu C, Tao H, Tian B et al (2016) Limited-irrigation improves water use efficiency and soil reservoir capacity through regulating root and canopy growth of winter wheat. Field Crops Res 196:268–275. https://doi.org/10.1016/j.fcr.2016.07.009
96. Xu J, Lowe C, Hernandez-Leon SG et al (2022) The Effects of Brief Heat During Early Booting on Reproductive, Developmental, and Chlorophyll Physiological Performance in Common Wheat (Triticum aestivum L). Front Plant Sci 13:886541. https://doi.org/10.3389/fpls.2022.886541
97. Zadoks JC, Chang TT, Konzak CF (1974) A decimal code for the growth stages of cereals. Weed Res 14:415–421. https://doi.org/10.1111/j.1365-3180.1974.tb01084.x
98. Zaman F, Hassan MU, Khattak WA et al (2024) The pivotal role of arbuscular mycorrhizal fungi in enhancing plant biomass and nutrient availability under drought stress conditions: A global meta-analysis. Sci Total Environ 955:176960. https://doi.org/10.1016/j.scitotenv.2024.176960
99. Zegada-Lizarazu W, Monti A (2019) Deep root growth, ABA adjustments and root water uptake response to soil water deficit in giant reed. Ann Bot 124:605–615. https://doi.org/10.1093/aob/mcz001
100. Zhao Y, Wang L, Chun KP et al (2024) Dynamic hydrological niche segregation: How plants compete for water in a semi-arid ecosystem. J Hydrol 630:130677. https://doi.org/10.1016/j.jhydrol.2024.130677
101. Zoomash Selhausen Annual Weather Averages (2025) In: World® Weather Online. https://www.worldweatheronline.com/selhausen-weather-averages/nordrhein-westfalen/de.aspx. Accessed 10 Mar

Figures

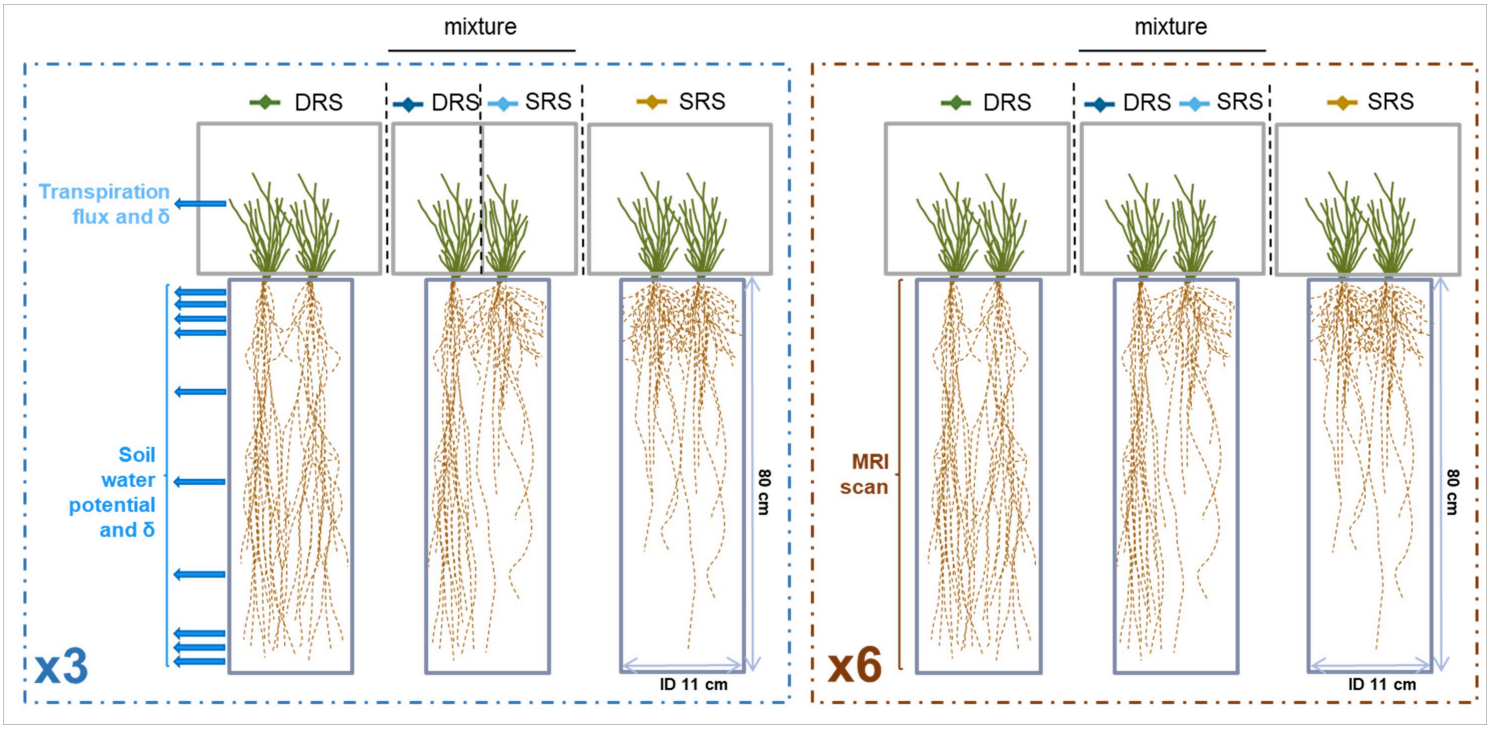

Figure 1

Diagram of the experiment with the three replicates of water treatments (well-watered "WW" vs. water deficit "WD") and plant modalities (DRS in monoculture, dark green; DRS in mixture, dark blue; SRS in mixture, light blue; SRS in monoculture, orange). Six additional column replicates per modality were grown in parallel to carry out additional physiological measurements above and below ground.

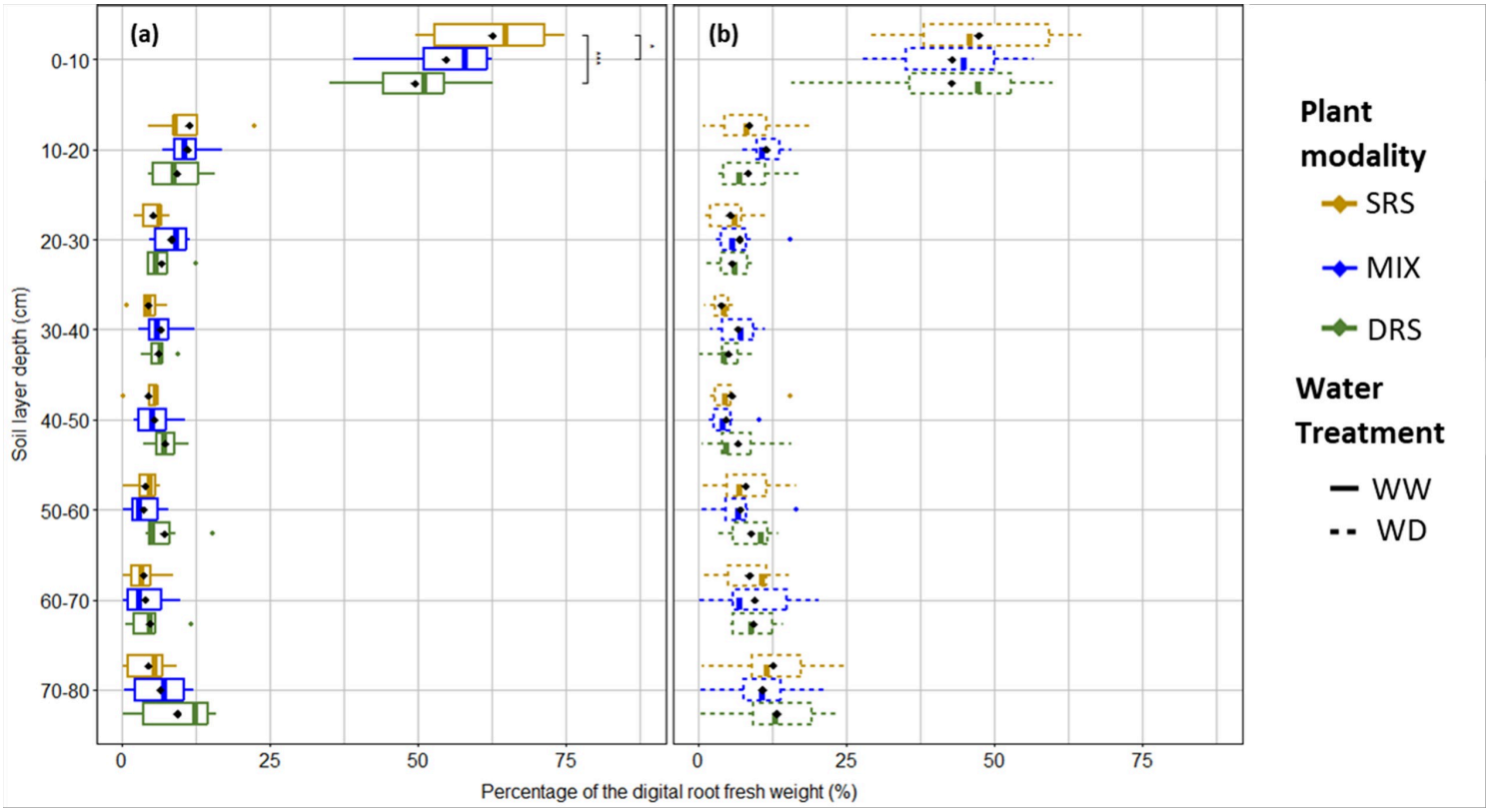

Figure 2

Distributions of the percentage of digital root fresh weight (DRFW) per 10 cm soil layer, measured in situ by MRI at 43 DaS for the well-watered (WW, lines, panel a) and water deficit (WD, dots, panel b) treatments among the plant modalities (DRS in monoculture, dark green; Mixture – MIX, blue; and SRS in monoculture, orange) (n=6).

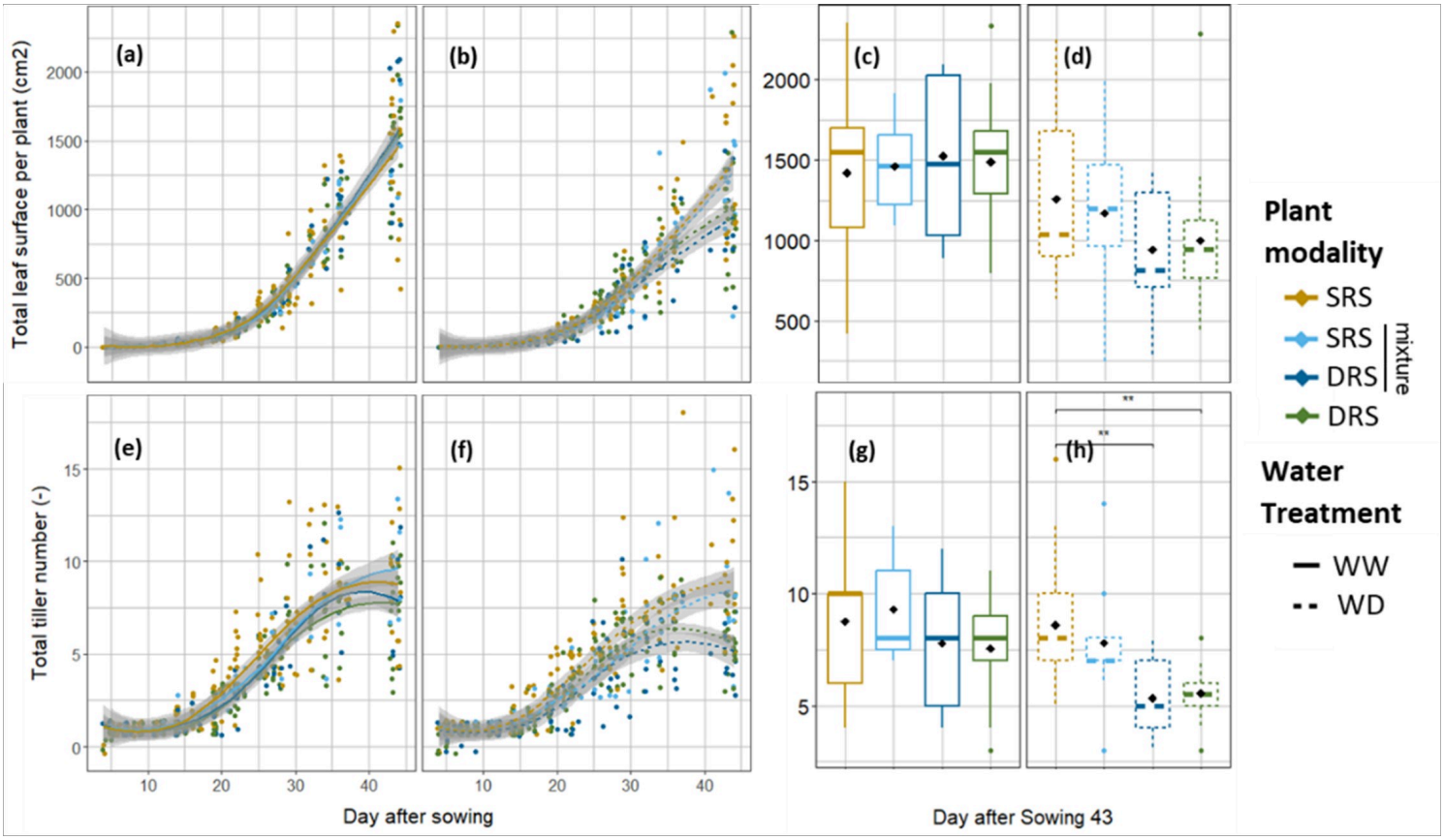

Figure 3

Total leaf area per plant (in cm^2, panels a, b, c, and d), and number of tiller per plant (panels e, f, g, and h) for the four plant modalities (DRS monoculture, dark green; DRS mixture, dark blue; SRS mixture, light blue; SRS monoculture, orange) under well-watered conditions (WW, lines, panels a, c, e and g) and water deficit (WD, dots, panels b, d, f and h), throughout growth, modelled by LOESS regression (Locally Estimated Scatterplot Smoothing, 95% confidence interval) (a, b, e and f) and at 43 DaS (c, d, g and h) (n = 18 for SRS and DRS in monoculture, n = 9 for SRS and DRS in mixture).

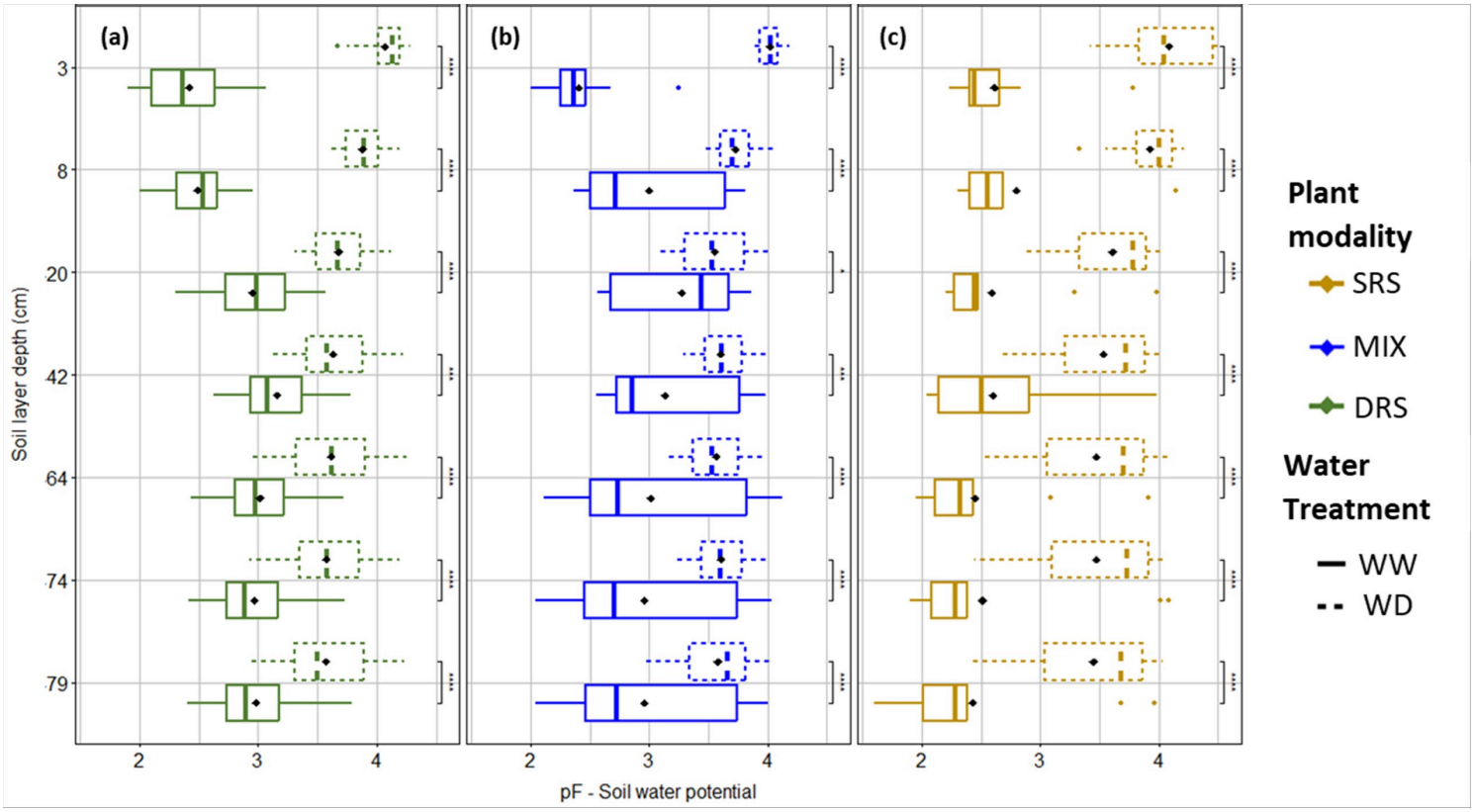

Figure 4

Soil depth profile distribution of water potential between 39 and 42 DaS, expressed as pF, for the well-watered (WW, lines) and water deficit (WD, dots) treatments among the plant modalities (DRS in monoculture, dark green, panel a; Mixture – MIX, blue, panel b; and SRS in monoculture, orange, panel c) (n=3).

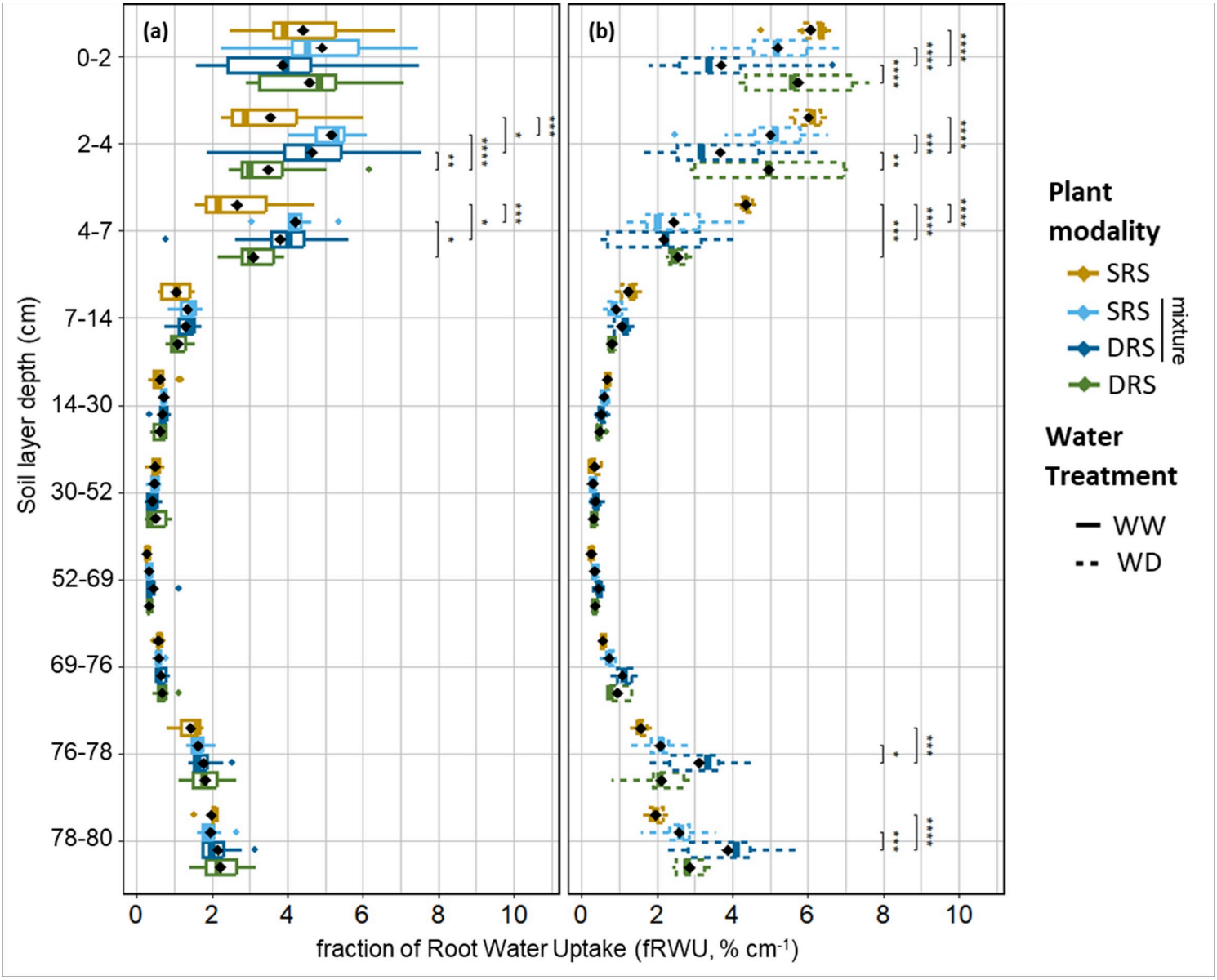

Figure 5

Fraction of the Root Water Uptake (fRWU, % cm^{-1}) distributions (panels a and b) and mean values (panels c and d) estimated between 39 and 42 DaS , for the four plant modalities (DRS in monoculture, dark green; DRS in mixture, dark blue; SRS in mixture, light blue; SRS in monoculture, orange), across ten soil layers (0-2; 2-4; 4-7; 7-14; 14-30; 30-52; 52-69; 69-76; 76-78; 78-80 cm) under well-watered (WW, lines, panels a) and water deficit (WD, dots, panels b) conditions (n=7-12).

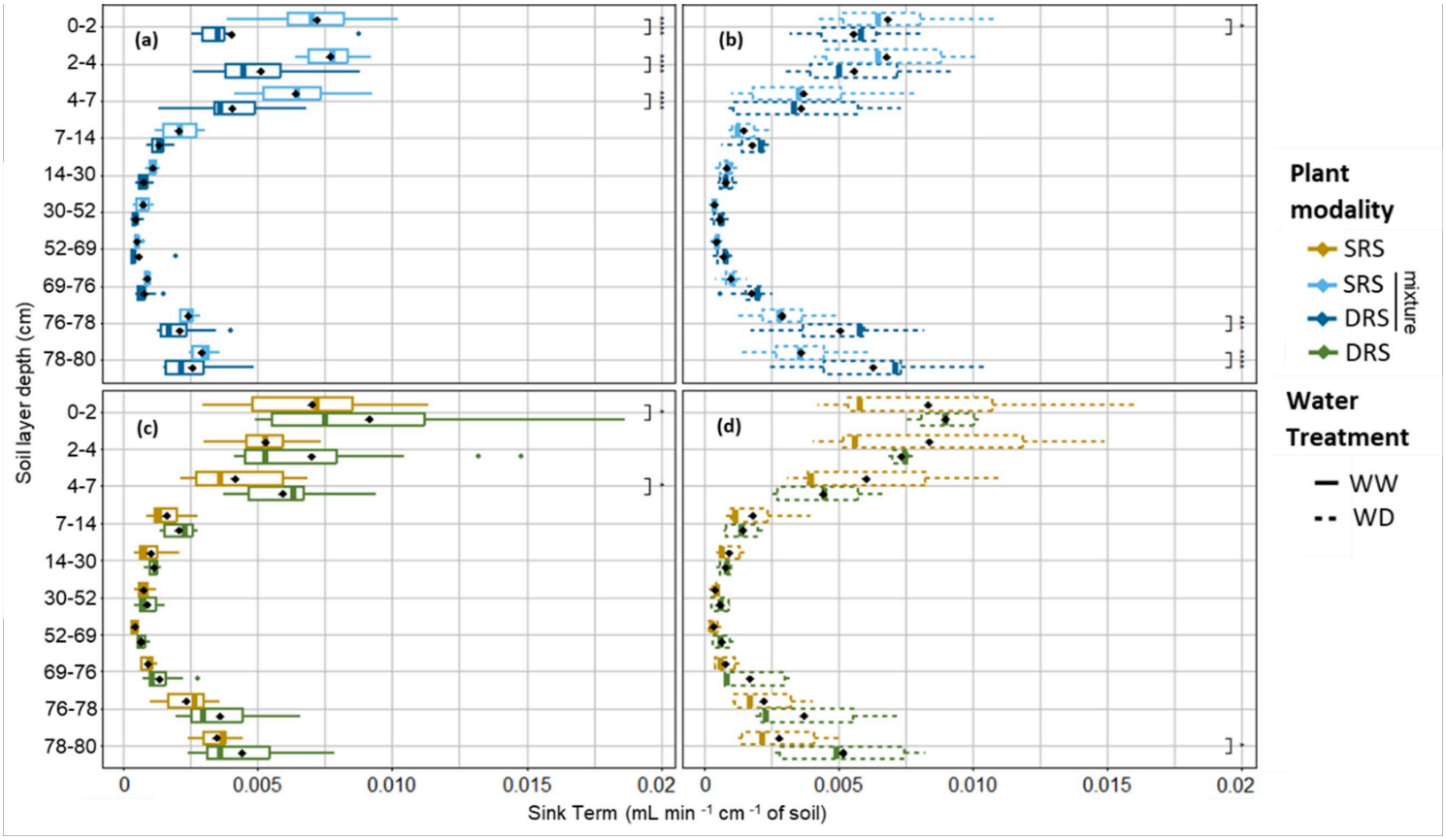

Figure 6

Distributions of the Sink Term (mL min^{-1} cm^{-1}) estimated between 39 and 42 DaS, for the four plant modalities (DRS in monoculture, dark green; DRS in mixture, dark blue; SRS in mixture, light blue; SRS in monoculture, orange), across ten soil layers (0-2; 2-4; 4-7; 7-14; 14-30; 30-52; 52-69; 69-76; 76-78; 78-80 cm) under well-watered conditions (WW, lines, panels a and c) and water deficit (WD, dots, panels b and d) (n=7-12).

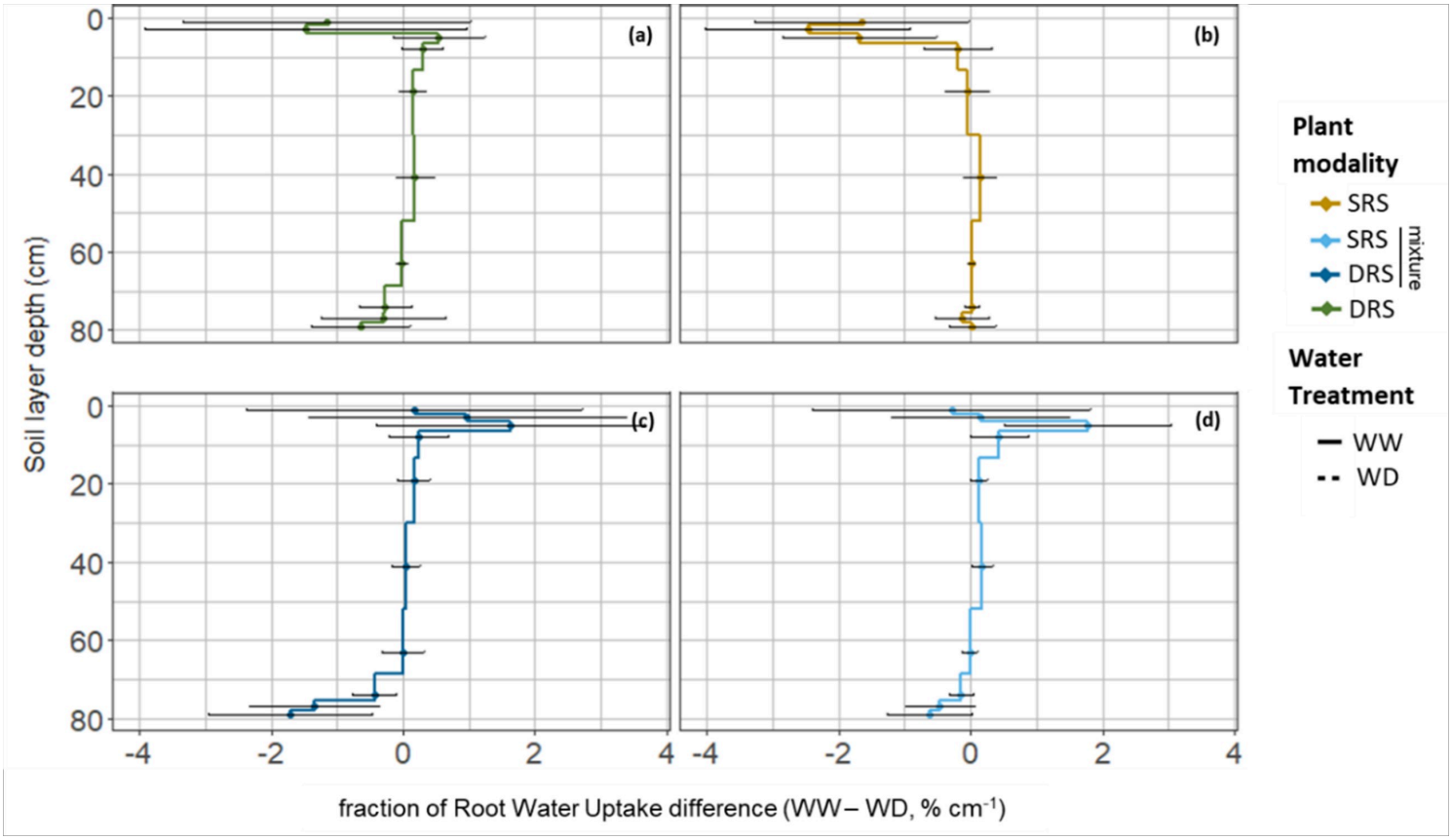

Figure 7

Differences of fraction of the Root Water Uptake (fRWU, % cm^{-1}) estimated between 39 and 42 DaS between water deficit (WD) and well-watered (WW) conditions for the four plant modalities (DRS in monoculture, dark green, panel a; SRS in monoculture, orange, panel b, DRS in mixture, dark blue, panel c; SRS in mixture, light blue, panel d), across ten soil layers (0-2; 2-4; 4-7; 7-14; 14-30; 30-52; 52-69; 69-76; 76-78; 78-80 cm). Standard deviations are indicated by black bars (n=3).

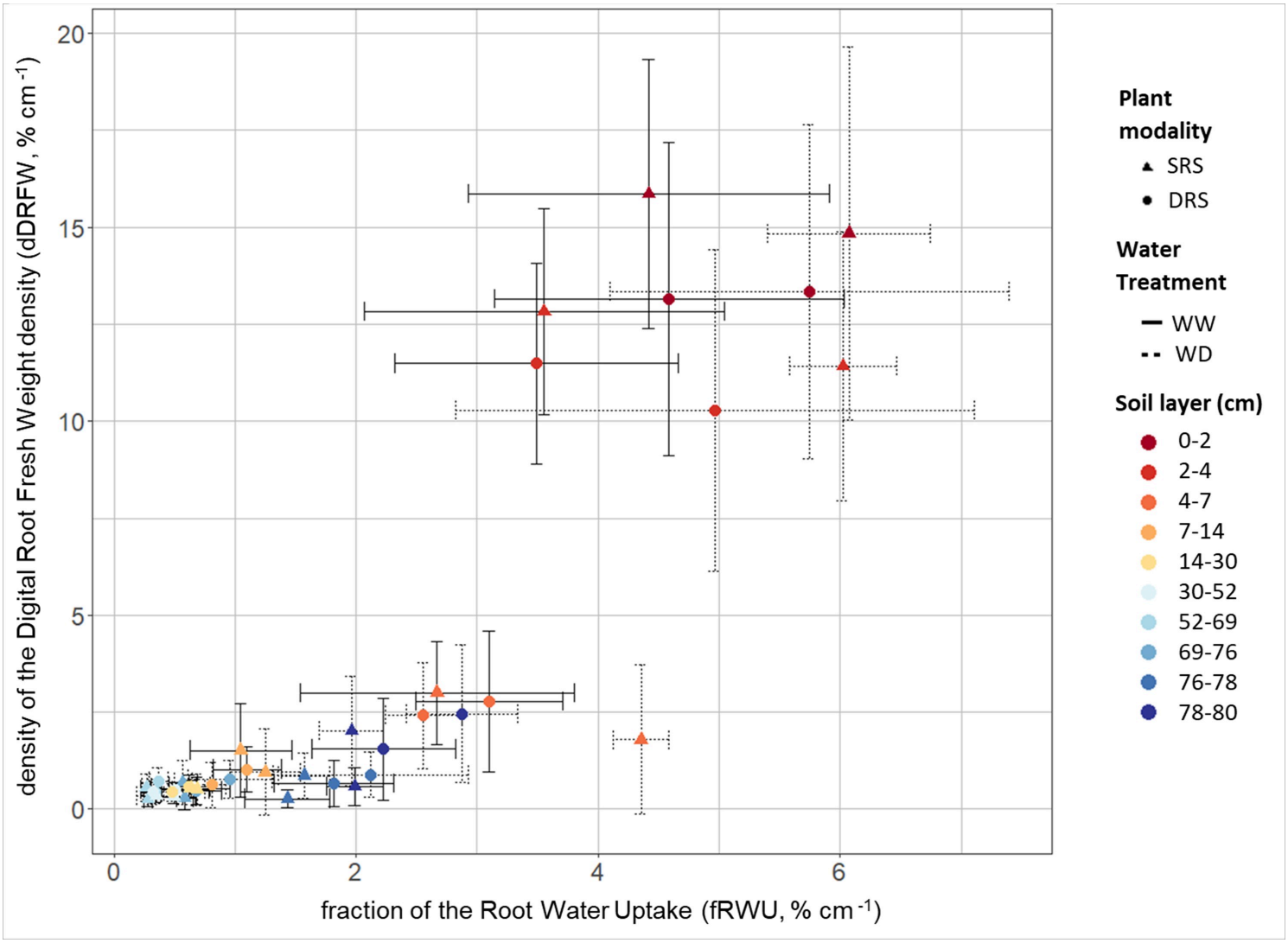

Figure 8

Density of the Digital Root Fresh Weight (dDRFW, % cm^{-1}, measured at 43 DaS) over the fraction of Root Water Uptake (fRWU, % cm^{-1}, estimated between 39 and 42 DaS). The points represent the average value of two plant modalities (DRS in monoculture, circle shape; SRS in monoculture, triangle shape), across ten soil layers (0-2; 2-4; 4-7; 7-14; 14-30; 30-52; 52-69; 69-76; 76-78; 78-80 cm) under well-watered conditions (WW, lines) and water deficit (WD, dots). Black bars indicate standard deviations.

Supplementary Files

This is a list of supplementary files associated with this preprint. Click to download.

- SupplementarymaterialLeGalletal.2025.docx